Original manuscript submitted to *Nature Communications*

Genome-wide targets identification by CRISPRi-Omics for high-titer production of free fatty acids in *Escherichia coli*

Lixia Fang[1,2], Jie Fan[1,2], Congya Wang[1,2], Yingxiu Cao[1,2] * & Hao Song[1,2] *

[1] Frontier Science Center for Synthetic Biology and Key Laboratory of Systems Bioengineering (Ministry of Education), Tianjin University, Tianjin 300072, China

[2] Collaborative Innovation Center of Chemical Science and Engineering (Tianjin), School of Chemical Engineering and Technology, Tianjin University, Tianjin 300072, China

* Correspondence and requests for materials should be addressed to Y.C. (caoyingxiu@tju.edu.cn) or H.S. (hsong@tju.edu.cn).

Abstract

To construct a superior microbial cell factory for chemical synthesis, a major challenge is to fully exploit cell potential via identifying and engineering beneficial gene targets in the sophisticated metabolic networks. Here, we develop an approach that integrates CRISPR interference (CRISPRi) to readily modulate genes expression and omics analyses to identify potential targets in multiple cellular processes, enabling systematical discovery of beneficial chromosomal gene targets that can be engineered to optimize free fatty acids (FFAs) production in *Escherichia coli*. We identify 56 beneficial genes via synergistic CRISPRi-Omics strategy, including 46 novel targets functioning in cell structure and division, and signaling transduction that efficiently facilitate FFAs production. Upon repressing *ihfA* and overexpressing *aidB* and *tesA'* in *E. coli*, the recombinant strain LihfA-OaidB results in a FFAs titer of 21.6 g L^{-1} in fed-batch fermentation, which, to our best knowledge, is the maximum FFAs titer by the recombinant *E. coli* reported to date.

Introduction

Microbial biosynthesis of a desired product is a sophisticated process, usually involving the coordination of multiple metabolic intermediates or reactions subject to complicated interactions[1,2]. On the one hand, each of these intermediates flows to other metabolic processes for biosynthesis of cellular components or metabolites, acting as one of the multi-branched nodes in the topology of metabolic landscapes[3]. On the other hand, each reaction in the biosynthetic pathway deeply rely on many cellular processes, such as genes transcription and translation to enable enzymes function[4-6], or cell proliferation to ensure biomass accumulation[7]. As such, manipulation of other metabolic pathways or cellular processes might lead to an unexpectedly improvement on the biosynthesis of a desired product due to distant effects of genetic modulations or unknown regulatory interactions[8,9]. Thus, to construct a superior microbial cell factory for an enhanced product biosynthesis, it is highly desirable to genome-widely identify beneficial gene targets in the highly complicated intracellular interaction networks that can be reengineered for this purpose. As such, the interwoven linkage mechanism between product biosynthesis and other sophisticated genetic and metabolic networks can be better understood.

Free fatty acids (FFAs) are feedstocks for the manufacture of detergents, lubricants, cosmetics, and pharmaceutical ingredients[10,11]. A number of metabolic engineering approaches were developed to facilitate FFAs production in *E. coli*. Overexpression of key enzymes in the FFAs biosynthetic pathway such as acetyl-coenzyme A (CoA)

53 carboxylase[12-14] and fatty acyl-ACP thioesterase[12,13,15-17], or deletion of key genes in
54 the beta-oxidation pathway such as *fadD*[12,13,15-17] or *fadE*[15] gene, were studied. In
55 particular, optimally combinatorial expression of 15 crucial genes in the FFAs
56 biosynthetic pathway with *fadD* deletion in *E. coli* BL21 resulted in a titer of 8.6 g L^{-1}
57 of FFAs[18]. However, the cell potential for FFAs overproduction is still not fully
58 unleashed via modulating the FFAs directly related metabolic pathways alone[19].
59 Besides, the cellular rewiring mechanism and the linkage between FFAs biosynthesis
60 and other cellular processes is still largely unknown, and it remains difficult in
61 systematically identifying beneficial gene targets using laborious and time-consuming
62 genome engineering methods, such as homologous recombination-based gene
63 knockout[20]. These hurdles severely restrict the speed and scope of engineering of
64 microbial hosts to obtain a superior overproducer.

65 Here, we employ a systems metabolic engineering strategy for rapid, systematical
66 and effective identification of chromosomal gene targets that can be engineered for
67 the enhanced production of FFAs in *E. coli*. This strategy makes use of both the
68 CRISPR interference (CRISPRi) that readily down-regulates genes expression in a
69 dose-dependent manner to rapidly identify beneficial knockdown targets, and the
70 omics analyses of different strains that allows acquisition of comprehensive data
71 related to mechanisms of cellular metabolism to dig potential targets in the genetic
72 and metabolic networks. By way of this synergistic CRISPRi–Omics strategy, we
73 identified 46 new beneficial gene targets that efficiently facilitate FFAs production,

which involves in cell division, signaling transduction and transport, cell structure, and other seemingly irrelevant cellular processes with FFAs biosynthesis. Upon repressing *ihfA* and overexpressing *aidB* and *tesA'*, the resulting recombinant *E. coli* strain LihfA-OaidB enabled a FFAs titer of 21.6 g L^{-1} (with productivity of 0.636 g L^{-1} h^{-1}) in fed-batch fermentation, which, to the best of our knowledge, is the maximally reported FFAs titer and productivity by the recombinant *E. coli* to date. Our findings not only allow for enhanced biosynthesis of the desired product, but also lead to a mechanistic understanding of the underlying linkage between product biosynthesis and multiple cellular processes.

Results

Construction of a non-toxic and functional CRISPRi system in *E. coli* BL21(DE3). CRISPRi system functioned through the expression of dCas9 and customized specific sgRNA[21] (**Supplementary Fig. 1a**). However, high-level dCas9 could cause a severe inhibition of cell growth and abnormal expression of genes in a strain-specific manner[22,23]. To determine a superior dCas9 expression level in BL21(DE3), we constructed plasmids with dCas9 being expressed under the control of the promoter P_{T7}, P_{T5}, P_{Trc} and P_{BAD}, respectively (**Supplementary Fig. 2a**). The expression strengths of these promoters were $P_{T7} > P_{T5} > P_{Trc} > P_{BAD}$, according to our previous study[24]. With green fluorescent protein (GFP) as a characterization signal driven by the P_{T7} promoter, fluorescence-based reporter plasmids were further

constructed (**Supplementary Fig. 2a**) and transformed into BL21(DE3), forming five strains G0 (P_{T7}-GFP), G1 (P_{T7}-GFP-P_{T7}-dCas9), G2 (P_{T7}-GFP-P_{T5}-dCas9), G3 (P_{T7}-GFP-P_{Trc}-dCas9), and G4 (P_{T7}-GFP-P_{BAD}-dCas9), respectively. We found that the OD_{600} and fluorescence level of the strains G1 and G2 were greatly decreased from the strain G0, while that of G3 and G4 were little affected compared with G0 (**Supplementary Fig. 1b**). This suggested that the expression of dCas9 at relatively low level, such as under the control of the P_{Trc} or P_{BAD} promoter, did not cause overt toxicity in our system.

Then, we examined the transcriptional repression capability of CRISPRi on gene expression by co-expressing a specific sgRNA. sgRNA-*gfp* was designed to target on the non-template strand of GFP at a position ~38 nucleotides downstream of the start codon to expect a high repression efficiency[25]. The plasmid Sg-Hgfp (**Supplementary Fig. 2b**), harboring sgRNA-*gfp* under the control of the P_R promoter, was constructed and transformed into the strains G0-G4, forming the strains g0-g4, respectively. The results showed that fluorescence levels of the strains co-expressing dCas9 and sgRNA-*gfp* (g1-g4) were all dramatically reduced in comparison to the corresponding strain expressing only dCas9 (G1-G4) (**Supplementary Fig. 1b**). It indicated that the CRISPRi system was functional for effective transcriptional repression. In addition, the strain with dCas9 regulated by the P_{Trc} promoter obtained the highest repression efficiency (93%) (**Supplementary Fig. 1b**). Thus, we selected

dCas9 controlled by the P_{Trc} promoter to construct the CRISPRi system in BL21(DE3).

Identification of beneficial gene targets in the pathways related to FFAs metabolism using CRISPRi system. Glycerol, serving as the substrate, is catabolized into key intermediates glyceraldehyde-3P, pyruvate, acetyl-CoA, malonyl-ACP in sequence and then converted into acyl-ACP through the fatty acid biosynthetic pathway (**Fig. 1a**). However, these key intermediates also involved in other metabolic pathways, resulting in diverted carbon fluxes away from FFAs. The expression of truncated fatty acyl-ACP thioesterase TesA' (with leader sequence deleted) could release free fatty acid intermediates from ACP in the cytosol[26,27]. Nevertheless, the synthetic FFAs are degraded naturally by the beta-oxidation process (**Fig. 1a**). To channel carbon flux towards FFAs and impede products' degradation, we chose 108 genes in the chromosome that related with the FFAs metabolism and regulation as candidate targets for modulation by CRISPRi, and classified them into five modules (upstream carbon flux diversion, downstream carbon flux diversion, amino acid metabolism, beta-oxidation, and transcription factors) (**Fig. 1a**).

To facilitate large-scale target identification, we constructed a library of 108 synthetic sgRNAs that repress the expression of the 108 genes in the above five modules with high silencing efficiency[21]. We introduced plasmids harboring each of the 108 synthetic sgRNAs individually into the starting strain CF co-expressing TesA'

and dCas9 in BL21(ED3) to implement gene perturbations (**Fig. 1b**). The strain CF transformed with plasmid Sg-0 that expressed sgRNA0 without target site complementary sequence was named as the strain Control, which produced FFAs with a tier of 631 mg L^{-1}. Any CRISPRi-engineered strain that could increase FFAs titer by more than 20% compared with the strain Control was sorted out. As a result, 30 beneficial targets were identified from the library and the highest production of FFAs reached 1,232 mg L^{-1}, 95% higher than that of the strain Control (**Fig. 2**).

The identified beneficial genes were almost evenly distributed in the modules of upstream carbon flux diversion (**Fig. 2a**), downstream carbon flux diversion (**Fig. 2b**), beta-oxidation (**Fig. 2d**), and transcription factors (**Fig. 2e**). It suggested that reducing the carbon flux that flows to the by-products phosphatidylglycerol (*gpsA*, *plsY*, *pgpB* and *pgpC*), D-Lactate (*dld*), acetate (*pta*, *yccX* and *eutE*) and biotin (*bioC*, *bioH* and *bioD*), or impeding fatty acids degradation (*fadE*, *fadB*, *atoB* and *yqeF*) contributed to the enhanced production of FFAs. Reducing the expression of a few transcription factors (including *fabR*, *fadR*, *asnC*, *fnr*, *cra*, *gadW*, *glcC*, *glpR*, *ihfA*, *ihfB* and *torR*) also enhanced the production of FFAs (**Fig. 2e**), which might benefit from their global regulation of genes expression. However, reducing amino acids biosynthetic pathways was unfavorable for FFAs production, as the engineered strains obtained decreased titer of FFAs or failed to be constructed (**Fig. 2c**). The possible reason was that these amino acids were necessary for cell viability, but the reduced amount of amino acids upon CRISPRi perturbation was insufficient to maintain normal cell physiology. Thus,

157 in addition to the key enzymes in the FFAs biosynthetic pathway, there exist many
158 chromosomal genes seemingly unrelated to FFAs that could be beneficial to the
159 enhanced FFAs production.

160 Then, we tuned repression efficiency towards each of the 30 beneficial genes to
161 optimize their individual expression level. sgRNAs were designed to bind the
162 non-template DNA strand at the middle or terminal region to achieve medium or low
163 repression efficiency towards each target[21] (**Fig. 3a**). The plasmids harboring each of
164 the 60 synthetic sgRNAs were thus individually introduced into the starting strain CF,
165 and the production titer of FFAs was determined, showing that 10 strains (LgpsA,
166 LpfkA, MyccX, LgabD, MgadA, MatoB, LatoB, LglpR, MihfA and LihfA) enabled
167 further improvement in FFAs production (**Fig. 3b**).

168 Among the 30 beneficial gene targets, 20 of them (*gpsA*, *plsY*, *pgpB*, *pgpC*, *dld*,
169 *yccX*, *bioC*, *bioH*, *bioD*, *gabD*, *gadA*, *asnC*, *fnr*, *cra*, *gadW*, *glcC*, *glpR*, *ihfA*, *ihfB*,
170 *torR*) were firstly engineered for FFAs production. We found three favorable
171 metabolic pathways that have not been studied or modulated for FFAs production
172 before, namely the biotin, phosphatidylglycerol, and glutamate biosynthetic pathways.
173 Even in pathways that have been modulated in previous studies, we also identified
174 novel beneficial targets, such as *dld* in the lactate biosynthetic pathway, *yccX* and
175 *eutE* in the acetate formation pathway. In particular, we found a few genes such as *pta*
176 in the acetate formation pathway that have been deleted in previous studies[28], which
177 however showed no promotional effect on FFAs production, while CRISPRi

perturbation of the *pta* expression in this study significantly enhanced FFAs production. Collectively, these results demonstrate that CRISPRi is of use for systematical identification of beneficial targets that can be engineered for improved biosynthesis of a desired product.

Identification of potential targets in the cellular network via proteome and transcriptome analyses. To explore more potential targets that could facilitate FFAs production, we further focused on transcription factors in consideration of their complicated regulation functions on metabolic networks. Among all the targeted transcription factors, repression of *ihfA* with low efficiency (named as the strain LihfA) achieved a highest FFAs production, followed by the strain HfadR that repressed *fadR* with high efficiency (**Figs. 2e** and **3b**). IhfA is the alpha subunit of the integration host factor (IHF) in *E. coli*, which is capable of affecting transcription on a genome-wide scale[29]. We found that down-regulation of *ihfA* could enhance FFAs production, and the FFAs titer was negatively correlated with the repression efficiency (**Fig. 4a**). Unlike IhfA, FadR controls the expression of several genes directly involved in fatty acid biosynthesis, degradation, and transport across cell membranes[30]. It is intriguing that up-regulation of FadR (named as the strain OfadR) could also increase the FFAs titer as demonstrated in a previous study[31] and this study (**Fig. 4a**).

Even though the strains with FFAs overproducing phenotype have different genotypes, these strains might have convergent regulatory responses that facilitate FFAs biosynthesis. Thus, the three above engineered strains (LihfA, HfadR and OfadR, with knockdown of *ihfA*, *fadR* and overexpression of *fadR*, respectively) with high-titer FFAs and the strain Control were applied for proteome and transcriptome analyses to investigate the underlying mechanism of cellular responses to genetic modulations. Cells were sampled at the early stationary phase (24 h upon IPTG induction) (**Supplementary Fig. 3**). Hundreds of genes and proteins were differentially expressed in each pair of LihfA vs. Control, HfadR vs. Control, and OfadR vs. Control (**Supplementary Figs. 4** and **5**), suggesting the global modulation of genes in the engineered strains. To identify convergent rewiring in these high-titer strains, we plotted the differentially expressed genes (DEGs) of the three pairs in a Venn diagram (**Fig. 4b**). As a result, 24 down-regulated targets and 17 up-regulated targets were selected based on their significantly differential expression at the protein level (a and c, respectively) or at the transcript level (b and d, respectively) in at least two pairs (**Fig. 4b**) (see details in Supplementary Materials). The differential expression levels of these 41 genes are summarized in **Fig. 4c**. These potentially favorable gene targets are newly identified and seemingly irrelevant to FFAs biosynthesis in a direct fashion.

To test the function of these 41 candidate targets on FFAs production, the corresponding reverse engineering of each gene was conducted. We applied CRISPRi

to repress the expression of the 24 'down-regulated' genes or utilized the P_{BAD} promoter to overexpress the 17 'up-regulated' genes (**Fig. 5a**). The plasmids carrying the cassettes towards each candidate gene were transformed into the starting strain CF. A FFAs assay of the resulting strains showed that modulation of the 19 genes among the identified targets enhanced FFAs production by more than 20% in comparison to the strain Control (**Fig. 5b**). Considering that the selected genes were all differentially expressed in the strain pair of LihfA vs. Control (**Fig. 4c**), these targets were also manipulated in the strain LihfA to test their effects on FFAs production (**Fig. 5c**). As a result, 13 engineered strains gained further increase in FFAs production compared with the strain LihfA (**Fig. 5d**). In particular, the highest FFAs production was obtained in the strain LihfA-OaidB, in which the *ihfA* gene was repressed with low silencing efficiency and the *aidB* gene was overexpressed under the P_{BAD} promoter. The titer is up to 2,052 mg L^{-1}, which is 57% and 225% higher than that of the strains LihfA and Control, respectively (**Fig. 5d**). In summary, 26 (*norR*, *nrdE*, *npr*, *yihU*, *glpG*, *ftsQ*, *creC*, *sdhB*, *pal*, *rplW*, *tyrU*, *crsC*, *rnpB*, *ssrS*, *csrB*, *ryfA*, *sdsR*, *folk*, *aidB*, *yphF*, *deoD*, *nnr*, *rihC*, *hofP*, ECD_01466, and *ulaE*) out of the 41 newly identified genes are determined as the beneficial targets, which are validated to enhance the FFAs production by reverse engineering.

Exploration of cellular processes facilitating FFAs production. The newly identified beneficial targets are not in the metabolic pathways that directly related to

FFAs biosynthesis. To mine out the related regulatory mechanisms for FFAs production, the functions of the 26 beneficial genes were analyzed according to bioinformatics analysis of the database (NCBI, KEGG, UniProt and Gene Ontology) and summarized into eight sets (**Fig. 6, Supplementary Table 1**). Based on the FFAs titer of the corresponding engineered strains, the weight value (W value) of each set was calculated to characterize their effects on the enhancement of FFAs production. The eight sets were arranged in descending order of W value as follows: cell division, transduction and transport, energy metabolism, cellular structure, non-coding RNAs (ncRNAs), protein metabolism, nucleic acid metabolism, and cofactor metabolism (**Fig. 6, Supplementary Table 1**). Surprisingly, the processes such as cell division, signal transduction, protein metabolism and nucleic acid metabolism seemingly not associated with FFAs biosynthesis in any previous studies that showed favorable effect on FFAs production. These results indicate that the manipulation of cellular processes that are seemingly irrelevant with FFAs biosynthesis can also remarkably boost FFAs production.

Then, we further dissect the underlying connections between these enriched cellular processes and FFAs production. Down-regulation of *ftsQ* or *pal* significantly increased the FFAs concentration, inactivation of which resulted in deficiency in cell division and formed long multi-septated cell chains[32,33], which might associated with the increased cell volumes for storing FFAs. Down-regulation of *creC*, a sensor for the early response to phosphate starvation[34], was favorable for enhanced FFAs

261 production, which is consistent with the promotive effects of phosphate limitation
262 cultivations[35]. The functioning of *npr* down-regulation and *yphF* up-regulation may
263 be associated with the reduction of nitrogen assimilation[36] and the elevation of
264 carbohydrates' uptake[37], indicating a regulatory link between nitrogen and carbon
265 utilization for the efficient FFAs production. Down-regulation of ATP-consuming
266 proteins (such as those encoded by the genes *norR*, *nrdE*, *creC* and *rplW*) indirectly
267 increased ATP availability, a potential bottleneck for FFAs biosynthesis[19]. Beneficial
268 effects from down-regulation of membrane proteins (such as those encoded by the
269 genes *glpG*, *ftsQ*, *creC* and *pal*) might associated with microbial tolerance to FFAs[38].
270 The functioning of down-regulation of *rplW* (encoding 50S ribosomal subunit protein
271 L23), *tyrU* (encoding tRNA-Tyr) and *rnpB* (encoding M1 RNA, catalytic component
272 of tRNA processing enzyme RNase P) was associated with the inhibition of protein
273 synthesis, which increased partitioning of total carbon to lipids[8]. Up-regulation of *nnr,*
274 facilitating the repair of NAD(P)H hydrates to NAD(P)H[39], could be an important
275 complement strategy in enhancing NADPH availability, which plays an important
276 role in FFAs production[19,40]. In all, these findings provide new insights into linkages
277 between cell functions and product biosynthesis, guiding avenues for further strain
278 development.

279 As a result, the engineered *E. coli* strain LihfA-OaidB with simultaneous repression
280 of *ihfA* and overexpression of *aidB* and *tesA'* achieved the highest titer of FFAs
281 production. According to the results of combined omics analyses and reverse

engineering, we concluded that down-regulation of *ihfA* induced comprehensive adjustments of cellular processes that promoted the FFAs production. Nevertheless, repression of *ihfA* might be unfavorable for cellular survival at acidic pH as IHF is required for the induction of acid resistance[41,42]. AidB, one of the DNA damage repairing protein in *E. coli*, is involved in adaptive response of cells, serving to protect cells from cytotoxic effects of acidified cytoplasm or alkylating agents[43-45]. Thus, we speculated that up-regulation of *aidB* in the strain LihfA reconciled the stress from the acidic environment posed by the produced FFAs, facilitating FFAs biosynthesis in the strain LihfA-OaidB.

Further enhancing FFAs production by fed-batch fermentation. To further enhance FFAs production of the recombinant strain LihfA-OaidB in a scaled-up process, fed-batch fermentations were performed in a 5 L fermenter, using the dO_2-stat feeding strategy (details described in Methods). With arabinose and IPTG induction, *aidB* (DNA alkylation damage repair protein) was overexpressed by the P_{BAD} promoter, *tesA'* (truncated acyl-CoA thioesterase) was overexpressed by the P_{T7} promoter and *ihfA* (integration host factor subunit alpha) was repressed by CRISPRi with low silencing efficiency in the strain LihfA-OaidB. The FFAs production and cell density of the recombinant strain LihfA-OaidB increased along with the glycerol consumption (**Fig. 7a**). When cells were cultivated for 34 h after IPTG induction, LihfA-OaidB produced a titer of 21.6 g L^{-1} FFAs, accompanied by 0.636 g L^{-1} h^{-1}

productivity and 0.146 g FFAs per gram glycerol yield, the highest production titer and productivity in *E. coli* reported to date[18,46]. Extracellularly secreted FFAs were clearly visible at the top of the culture medium after centrifugation (**Fig. 7b**). Moreover, floating dead cells or fatty acid particles[47] were precipitated and stuck on the fermenter inner wall and sensors over the course of the fermentation process (**Supplementary Fig. 6**), exhibiting an additional production of FFAs that is however hard to accurately quantify and not counted in the FFAs titer. Thus, the overall actual FFAs production was higher than that showed in **Fig. 7a**.

Discussion

Genome-scale identification of beneficial gene targets in the chromosome for improving production of a desired product is challenging due to the complicated intracellular interactions. We here developed a systems metabolic engineering approach, which took the advantage of CRISPRi to readily and rapidly down-regulate gene expression and the omics analyses to provide potential targets in the cellular interaction network, thus enabling rapid, systematical and effective identification of beneficial targets that can be engineered to optimize FFAs production in *E. coli*. This synergistic strategy integrated the 'forward' and 'reverse' metabolic engineering cycles and their interaction[48] (**Supplementary Fig. 7**). In forward metabolic engineering, CRISPRi-mediated gene down-regulation functions were pursued in this work for the identification of beneficial chromosomal targets in the competitive or

324 regulatory pathways of FFAs biosynthesis that can be repressed in high, intermediate
325 and low levels, unlike gene knockout, to enhance FFAs production. In reverse
326 metabolic engineering, proteome and transcriptome analyses of the strains with
327 differential FFAs production provide comprehensive data related to mechanisms of
328 cellular metabolism, which can be validated experimentally via CRISPRi system and
329 plasmid mediated expression system. In doing so, we identified beneficial targets that
330 even seemingly irrelevant with FFAs biosynthesis, which are generally inaccessible to
331 hypothesis-driven or random gene targeting, aiding in expanding hosts' potential of
332 enhanced products synthesis. To our knowledge, this is the first report that
333 systematically identifies beneficial target genes in the cellular interaction network for
334 enhanced FFAs biosynthesis.

335 Many new approaches, including in vitro reconstitution of enzymes in the FFAs
336 biosynthetic pathway[49,50], engineering the reversal of the beta-oxidation pathway[51],
337 and construction of malonyl-CoA sensors[52,53], have been studied to enhance FFAs
338 production in *E. coli*. However, these approaches essentially focused on the
339 optimization of FFAs metabolic pathways alone, not exploiting the full potential of
340 interwoven intracellular processes. In our study, gene perturbations on the cellular
341 interaction network, including the competitive pathways of FFAs biosynthesis,
342 transcription factors and cellular processes that seemingly irrelevant with FFAs
343 metabolism, were systematically investigated to unleash the cellular potential and
344 change the cells towards a state of FFAs overproduction. As a result, the best

345 engineered strain LihfA-OaidB produced FFAs with a titer of 21.6 g L^{-1} (0.636 g L^{-1}
346 h^{-1} productivity) under fed-batch conditions, which, to the best of our knowledge, is
347 the maximally reported FFAs titer and productivity by recombinant *E. coli* to date.
348 Furthermore, the potential of the identified beneficial targets and our constructed
349 strains for improving FFAs production could be further integrated and amplified by
350 combinatorial genetic perturbations[54] and exploiting nongenetic variation[46].

351 Beneficial targets that were identified by our synergistic CRISPRi-Omics strategy
352 participate in diverse cellular processes, which support the idea that product synthesis
353 is a complex process and that global optimization of cellular machinery is required for
354 optimized product synthesis. Generally, these targets primarily associate with
355 metabolic processes, other cellular processes or regulatory elements. As to metabolic
356 processes, we identified novel beneficial targets in the common targeted pathways,
357 such as *yccX* and *eutE* in acetate formation pathway, ATP-consuming protein *nrdE*
358 and NAD(P)H-hydrate repair enzyme *nnr*, as well as novel pathways that have not
359 been engineered for FFAs production such as the biotin biosynthetic pathway (*bioC*,
360 *bioH* and *bioD*). Our target screening approach also emphasizes the importance of
361 other cellular processes or functions in the strain improvement for optimized FFAs
362 production, such as cell division (*ftsQ* and *pal*) related morphology, signaling
363 transduction (*creC*) and transport (*npr* and *yphF*) related resources utilization, cellular
364 structure (*glpG*, *ftsQ* and *pal*) related cellular tolerance, protein metabolism (*rplW*,
365 *tyrU*, *rnpB*) related resources partition, and nucleic acid metabolism (*aidB*) related

adaptive response. In addition, we also identified beneficial regulatory elements that have not been engineered for FFAs production, such as the integration host factor *ihfA*, or novel ncRNAs *ryfA* and *sdsR*, which modulate FFAs production through regulation of multiple cellular processes. Thus, our findings provide insights into connections between FFAs biosynthesis and other cellular processes and expand the underlying mechanistic understanding of the regulation of FFAs production in *E. coli*.

Strains obtained through the identification and modulation of genes have proven to be a versatile and robust approach for improved FFAs production, which also offers avenues for engineering more potential targets for further improvement. Knowledge acquired in this work toward understanding the FFAs biosynthetic machinery can be extended to other microorganisms for FFAs production, such as yeast and oleaginous bacteria. The approach for identifying promising modulation candidates is also applicable to other products without obvious screening phenotypes.

In summary, the synergistic CRISPRi-Omics strategy enabling rapid, systematical and effective identification of beneficial targets in the intracellular interaction network provides novel insights and solutions for further increasing productivity of microbial cell factories and better understanding of the link between product biosynthesis and the other processes of cellular machinery.

Methods

Experimental materials. Strains and plasmids used in this study are listed in **Supplementary Table 2** and **Supplementary Table 3**, respectively. *E. coli* *Trans*1-T1 strain was used for cloning. *E. coli* BL21(DE3) and its derived strains were used for fermentation. Plasmids pACYCDuet-1, YX210, YX212 and YX213 were used as the vector for expression of dCas9, GFP or TesA'. Plasmid Sg-S (with two BsaI restriction sites) was constructed and used as a platform vector for expression of various sgRNAs. Plasmid Sg-BAD was used as the vector for expression of chromosome genes. Plasmids, except that for sgRNAs expression, were constructed by standard enzyme digestion and ligation. Target site complementary sequences of sgRNAs were designed according to previous studies[55]. Custom-designed spacers were inserted into plasmid Sg-S by one-step Golden Gate assembly[56,57], allowing rapid construction of plasmids for expression sgRNAs targeting any genomic locus of interest. Primers annealed to custom-designed spacers and primers used to amplify genes from *E. coli* genomic DNA were listed in **Supplementary Tables 4-7** and **Supplementary Table 8**, respectively. Codon-optimized genes were listed in **Supplementary Table 9**.

Culturing conditions and mediums. To assess FFAs production by different recombinant *E. coli* strains, fermentation was performed in glass tubes. Each strain was inoculated from a freshly transformed single colony in LB agar plate to 2 mL LB medium as seed culture. When cell accumulation reached to stationary phase, 1%

407 (V/V) of seed culture was re-inoculated to 5 mL modified M9 medium in glass tube.
408 The tube cultures then were induced with 1 mM IPTG when OD_{600} reached ~1.0 and
409 allowed to grow for an additional 40 h at 30°C and 220 rpm. When the P_{BAD} promoter
410 was applied, 10 mM arabinose was utilized to induce gene expression at OD_{600} 0.5–
411 0.6. All tube experiments were performed at least in triplicate. Flask fermentation of
412 50 mL culture broth was implemented for proteome and transcriptome analyses with
413 the identical culturing procedures of tube fermentation. M9 medium used for tube and
414 flask fermentation was as described by Schirmer et al. [58] with some modifications:
415 17.1 g L^{-1} $Na_2HPO_4 \cdot 12H_2O$, 3 g L^{-1} KH_2PO_4, 0.5 g L^{-1} NaCl, 2 g L^{-1} NH_4Cl, 2 g L^{-1}
416 yeast extract, 3% glycerol, 0.25 g L^{-1} $MgSO_4 \cdot 7H_2O$, 11.1 mg L^{-1} $CaCl_2$, 10 mg L^{-1}
417 thiamine and 0.1% (v/v) Triton-X100. 1 mL L^{-1} metal trace stock solution was also
418 supplemented, which contained 27 g L^{-1} $FeCl_3 \cdot 6H_2O$, 2 g L^{-1} $ZnCl_2$, 2 g L^{-1}
419 $Na_2MoO_4 \cdot 2H_2O$, 1.9 g L^{-1} $CuSO_4 \cdot 5H_2O$, 0.5 g L^{-1} H_3BO_3. pH was adjusted to about
420 7.2 by Tris. If necessary, 100 μg mL^{-1} carbenicillin or 34 μg mL^{-1} chloramphenicol
421 was supplemented.

422 For fed-batch fermentation, an overnight LB culture (2 mL) of the freshly
423 transformed single colony was sub-cultured into 200 mL modified mineral medium (6
424 g L^{-1} NH_4Cl, 8.5 g L^{-1} KH_2PO_4, 0.5 g L^{-1} citrate, 5 g L^{-1} yeast extract, 15 g L^{-1}
425 glycerol, 1 g L^{-1} $MgSO_4 \cdot 7H_2O$, 0.07 g L^{-1} $CaCl_2 \cdot 2H_2O$, 4 mL L^{-1} metal trace stock
426 solution, 100 mg L^{-1} thiamine)[59] with 100 μg mL^{-1} carbenicillin and 34 μg mL^{-1}
427 chloramphenicol. When OD_{600} reached to 3-4, the cultured cells were re-inoculated

428 into a 5 L bioreactor (T&J, China) with 1.8 L modified mineral medium as above.
429 Fermentation temperature was set at 30°C and pH was controlled at 7 by feeding 6 N
430 ammonium hydroxide via an auto pump. Air flow rate was maintained at around 2 L
431 min^{-1}. The dissolved oxygen (dO_2) concentration was controlled above 30% by
432 agitation cascade (300–800 r.p.m). When cell density reached about 6 and 15, 10 mM
433 arabinose and 1 mM IPTG was added into the fermentation cell culture, respectively.
434 Feeding medium (2.47 g L^{-1} $MgSO_4 \cdot 7H_2O$, 500 g L^{-1} glycerol and 100 g L^{-1} yeast
435 extract) was fed to the fermentation culture after the initial 15 g L^{-1} glycerol was
436 almost depleted and the dissolved oxygen showed a sharp increase. The carbon source
437 restriction strategy was carried out by dO_2 concentration, given that the dO_2 level
438 immediately spiked once the carbon source was run out. Once the $dO_2 > 60\%$, the
439 feeding would automatically start at 5 mL min^{-1} until $dO_2 < 60\%$. Antifoam (Sigma)
440 was added automatically as needed. Broth samples (~5 ml) were collected at a series
441 of time points to measure cell density and stored at −20°C for further measurements
442 of residual glycerol and FFAs production.
443
444 **GFP Fluorescence assay.** Fluorescence signal of GFP was used to characterize
445 repression efficiency of the CRISPRi system. Culturing procedures and induction
446 process of the GFP reporting strains were the same as tube fermentation of the FFAs
447 producing strains. For each tube, 200 μL of sample was diluted into the linear range
448 of the detector with phosphate buffered saline (PBS) after IPTG induction for 20 h.

449 Fluorescence intensity (excitation at 485 nm and emission at 520 nm) and cell density
450 (OD_{600}) were detected using 96-well polystyrene plates (black plate with a clear
451 bottom) (Corning Incorporated 3603, USA) and a microplate reader (SpectraMax M2,
452 Molecular Devices, USA). The relative fluorescence intensity was first normalized
453 using OD_{600} and then subtracted that of blank *E. coli* BL21 (DE3). Experiments were
454 performed in triplicate.
455
456 **Metabolite extraction and analysis.** FFAs titers in whole-cell culture (only FFAs
457 was measured in this study) were quantified following previously published
458 methods[60]. Specifically, 0.5 ml of cell culture (or an appropriate volume of cell
459 culture diluted to 0.5 ml) was acidified with 50 μL of concentrated HCl, spiked with
460 60 μg of heptadecanoic acid as internal standard. The cell culture was extracted twice
461 with 0.5 ml of ethyl acetate. The extracted FFAs were then determined using a
462 Thermo Scientific TRACE 1300 gas chromatograph (GC) equipped with a
463 TG-WaxMS A column (30 m × 0.32 mm × 0.25 μm; Thermo Scientific) and a Flame
464 Ionization Detector (FID) operating under constant flow rate of the carrier gas
465 (nitrogen) at 1 mL min^{-1}. The following temperature program was used: hold at 50°C
466 for 1 min, then heat to 245°C at 30°C min^{-1} and hold at this temperature for 22.5 min.
467 Individual fatty acid species were qualified by authentic homologous standards and
468 quantified by comparing the peak areas with that of the internal standard using the

469 Chromeleon 7.1 software. Total concentrations of free fatty acids were calculated as
470 the sum of C_{12} to C_{18} (saturated and monounsaturated).
471 Glycerol concentration was determined by high-performance liquid
472 chromatography (HPLC) following Waters standard protocols. Briefly, filtered
473 culture supernatants were analyzed by a Waters HPLC system including a Waters
474 e2695 separation module, a Waters 2414 refractive index detector (RID) and an
475 Aminex HPX-87H column (Bio-Rad). The separation was performed through elution
476 with 5 mM H_2SO_4 at a flow rate of 0.6 mL min^{-1} at 65°C for 30 min.
477
478 **Proteome analysis.** Cells were harvested by centrifugation at 5000 rpm for 5 min at
479 24 h after IPTG induction and flash frozen with liquid nitrogen. For protein
480 preparation, cells were resuspended in 600 μL lysis buffer (0.05 M Tris, pH 8, 1%
481 SDS, and 8 M Urea) and disrupted by ultrasonication for 5 min (cycles with 2s work
482 and 3s pause). After centrifugation at 13000 rpm and 4°C for 20 min, the supernatant
483 was subjected to protein precipitation by adding pre-cooled acetone with 10 mM DTT.
484 The total precipitate was collected, dried and then re-dissolved in 600 μL Urea buffer
485 (0.05 M Tris, pH 8, and 8 M Urea). The protein samples were quantitated by the
486 Bradford method and qualitated by SDS-PAGE. A total of 100 μg of each sample was
487 trypsin-digested overnight and labeled using 4-plex iTRAQ reagents (AB SCIEX) as
488 manual described. The tryptic peptides corresponding to each sample were labeled

with its unique iTRAQ tags and proteomics analysis was conducted using a Triple TOF 6600 system (AB SCIEX). The data were analyzed by Novogene.

Transcriptome analysis. Cells were harvested after 24 h of IPTG induction by quick centrifugation at 10000 g for 1 min and immediately frozen in liquid nitrogen. Total RNA was extracted using the RNAprep pure Cell/Bacteria Kit (Tiangen) following lysozyme treatment. RNA degradation and contamination were monitored on 1 % agarose gels. RNA concentration was measured by Qubit® RNA Assay Kit in Qubit® 2.0 Flurometer (Life Technologies, CA, USA) and RNA integrity was assessed on a 2100 Bioanalyzer (Agilent Technologies, CA, USA). rRNA is removed using a Ribo-zero kit that leaves the mRNA. A total of 3 μg RNA was used as an input per sample. Sequencing libraries were generated using a NEBNext®UltraTM RNA Library Prep Kit for Illumina® (NEB, USA) following the manufacturer's instructions, and index codes were added to attribute sequences to each sample. Clustering of the index-coded samples was performed on a cBot Cluster Generation System using the TruSeq PE Cluster Kit v3-cBot-HS (Illumina) according to the manufacturer's instructions. After cluster generation, the library preparations were sequenced on an Illumina Hiseq 4000 platform and paired-end reads were generated. After these steps, the data were analyzed by Novogene.

Data availability

510 A reporting summary for this article is available as a Supplementary Information file.

511 The data that support the findings of this study are available from the corresponding

512 author upon request. The source data underlying Figs. 2a-e, 3b, 4a-c, 5b, 5d, 6, and 7a,

513 Supplementary Figs. 1b, 3, 4, and 5 and Supplementary Table 1 are provided as a

514 Source Data file.

References

1. Keasling, J. D. Manufacturing molecules through metabolic engineering. *Science* **330**, 1355-1358 (2010).
2. Nielsen, J. & Keasling, J. D. Engineering Cellular Metabolism. *Cell* **164**, 1185-1197 (2016).
3. Nielsen, J. It is all about metabolic fluxes. *Journal of Bacteriology* **185**, 7031-7035 (2003).
4. Li, G. W., Burkhardt, D., Gross, C. & Weissman, J. S. Quantifying Absolute Protein Synthesis Rates Reveals Principles Underlying Allocation of Cellular Resources. *Cell* **157**, 624-635 (2014).
5. Cambray, G., Guimaraes, J. C. & Arkin, A. P. Evaluation of 244,000 synthetic sequences reveals design principles to optimize translation in Escherichia coli. *Nature Biotechnology* **36**, 1005-+ (2018).
6. Gill, R. T., Valdes, J. J. & Bentley, W. E. A Comparative Study of Global Stress Gene Regulation in Response to Overexpression of Recombinant Proteins in Escherichia coli. *Metabolic Engineering* **2**, 178-189 (2000).
7. Boer, V. M., Crutchfield, C. A., Bradley, P. H., Botstein, D. & Rabinowitz, J. D. Growth-limiting Intracellular Metabolites in Yeast Growing under Diverse Nutrient Limitations. *Molecular Biology of the Cell* **21**, 198-211 (2010).
8. Ajjawi, I. et al. Lipid production in Nannochloropsis gaditana is doubled by decreasing expression of a single transcriptional regulator. *Nat Biotechnol* **35**, 647-652 (2017).
9. Huang, M., Bao, J., Hallstrom, B. M., Petranovic, D. & Nielsen, J. Efficient protein production by yeast requires global tuning of metabolism. *Nat Commun* **8**, 1131 (2017).
10. Tee, T. W., Chowdhury, A., Maranas, C. D. & Shanks, J. V. Systems metabolic engineering design: fatty acid production as an emerging case study. *Biotechnol Bioeng* **111**, 849-857 (2014).
11. Janssen, H. J. & Steinbuchel, A. Fatty acid synthesis in Escherichia coli and its applications towards the production of fatty acid based biofuels. *Biotechnol Biofuels* **7**, 7 (2014).
12. Lu, X., Vora, H. & Khosla, C. Overproduction of free fatty acids in E. coli: implications for biodiesel production. *Metab Eng* **10**, 333-339 (2008).
13. Lennen, R. M., Braden, D. J., West, R. A., Dumesic, J. A. & Pfleger, B. F. A process for microbial hydrocarbon synthesis: Overproduction of fatty acids in Escherichia coli and catalytic conversion to alkanes. *Biotechnol Bioeng* **106**, 193-202 (2010).
14. Lee, S., Jeon, E., Yun, H. S. & Lee, J. Improvement of Fatty Acid Biosynthesis by Engineered Recombinant Escherichia coli. *Biotechnology and Bioprocess Engineering* **16**, 706-713 (2011).

15. Steen, E. J. et al. Microbial production of fatty-acid-derived fuels and chemicals from plant biomass. *Nature* **463**, 559-562 (2010).
16. Choi, Y. J. & Lee, S. Y. Microbial production of short-chain alkanes. *Nature* **502**, 571-574 (2013).
17. Zhang, X. J., Li, M., Agrawal, A. & San, K. Y. Efficient free fatty acid production in Escherichia coli using plant acyl-ACP thioesterases. *Metabolic Engineering* **13**, 713-722 (2011).
18. Xu, P. et al. Modular optimization of multi-gene pathways for fatty acids production in E. coli. *Nat Commun* **4**, 1409 (2013).
19. He, L. et al. Central metabolic responses to the overproduction of fatty acids in Escherichia coli based on 13C-metabolic flux analysis. *Biotechnol Bioeng* **111**, 575-585 (2014).
20. Datsenko, K. A. & Wanner, B. L. One-step inactivation of chromosomal genes in Escherichia coli K-12 using PCR products. *Proceedings of the National Academy of Sciences of the United States of America* **97**, 6640-6645 (2000).
21. Qi, L. S. et al. Repurposing CRISPR as an RNA-guided platform for sequence-specific control of gene expression. *Cell* **152**, 1173-1183 (2013).
22. Cho, S. et al. High-Level dCas9 Expression Induces Abnormal Cell Morphology in Escherichia coli. *ACS Synth Biol* **7**, 1085-1094 (2018).
23. Cui, L. et al. A CRISPRi screen in E. coli reveals sequence-specific toxicity of dCas9. *Nat Commun* **9**, 1912 (2018).
24. Cao, Y. X. et al. Biosynthesis of odd-chain fatty alcohols in Escherichia coli. *Metab Eng* **29**, 113-123 (2015).
25. Cao, Y., Li, X., Li, F. & Song, H. CRISPRi-sRNA: Transcriptional-Translational Regulation of Extracellular Electron Transfer in Shewanella oneidensis. *ACS Synth Biol* **6**, 1679-1690 (2017).
26. Jiang, P. & Cronan, J. E., Jr. Inhibition of fatty acid synthesis in Escherichia coli in the absence of phospholipid synthesis and release of inhibition by thioesterase action. *J Bacteriol* **176**, 2814-2821 (1994).
27. Cho, H. & Cronan, J. E., Jr. Defective export of a periplasmic enzyme disrupts regulation of fatty acid synthesis. *J Biol Chem* **270**, 4216-4219 (1995).
28. Li, M., Zhang, X., Agrawal, A. & San, K. Y. Effect of acetate formation pathway and long chain fatty acid CoA-ligase on the free fatty acid production in E. coli expressing acy-ACP thioesterase from Ricinus communis. *Metab Eng* **14**, 380-387 (2012).
29. Prieto, A. I. et al. Genomic analysis of DNA binding and gene regulation by homologous nucleoid-associated proteins IHF and HU in Escherichia coli K12. *Nucleic Acids Research* **40**, 3524-3537 (2012).
30. Fujita, Y., Matsuoka, H. & Hirooka, K. Regulation of fatty acid metabolism in bacteria. *Mol Microbiol* **66**, 829-839 (2007).
31. Zhang, F. et al. Enhancing fatty acid production by the expression of the regulatory transcription factor FadR. *Metab Eng* **14**, 653-660 (2012).

32. van den Ent, F. et al. Structural and mutational analysis of the cell division protein FtsQ. *Mol Microbiol* **68**, 110-123 (2008).
33. Gerding, M. A., Ogata, Y., Pecora, N. D., Niki, H. & de Boer, P. A. The trans-envelope Tol-Pal complex is part of the cell division machinery and required for proper outer-membrane invagination during cell constriction in E. coli. *Mol Microbiol* **63**, 1008-1025 (2007).
34. Baek, J. H., Kang, Y. J. & Lee, S. Y. Transcript and protein level analyses of the interactions among PhoB, PhoR, PhoU and CreC in response to phosphate starvation in Escherichia coli. *FEMS Microbiol Lett* **277**, 254-259 (2007).
35. Youngquist, J. T., Rose, J. P. & Pfleger, B. F. Free fatty acid production in Escherichia coli under phosphate-limited conditions. *Appl Microbiol Biotechnol* **97**, 5149-5159 (2013).
36. Pfluger-Grau, K. & Gorke, B. Regulatory roles of the bacterial nitrogen-related phosphotransferase system. *Trends Microbiol* **18**, 205-214 (2010).
37. Schneider, E. ABC transporters catalyzing carbohydrate uptake. *Res Microbiol* **152**, 303-310 (2001).
38. Rodriguez-Moya, M. & Gonzalez, R. Proteomic analysis of the response of Escherichia coli to short-chain fatty acids. *J Proteomics* **122**, 86-99 (2015).
39. Marbaix, A. Y. et al. Extremely Conserved ATP- or ADP-dependent Enzymatic System for Nicotinamide Nucleotide Repair. *Journal of Biological Chemistry* **286**, 41246-41252 (2011).
40. Li, W., Wu, H., Li, M. & San, K. Y. Effect of NADPH availability on free fatty acid production in Escherichia coli. *Biotechnol Bioeng* **115**, 444-452 (2018).
41. Bi, H. & Zhang, C. Integration host factor is required for the induction of acid resistance in Escherichia coli. *Curr Microbiol* **69**, 218-224 (2014).
42. Aquino, P. et al. Coordinated regulation of acid resistance in Escherichia coli. *BMC Syst Biol* **11**, 1 (2017).
43. Smirnova, G. V., Oktyabrsky, O. N., Moshonkina, E. V. & Zakirova, N. V. Induction of the alkylation-inducible aidB gene of Escherichia coli by cytoplasmic acidification and N-ethylmaleimide. *Mutat Res* **314**, 51-56 (1994).
44. Bowles, T., Metz, A. H., O'Quin, J., Wawrzak, Z. & Eichman, B. F. Structure and DNA binding of alkylation response protein AidB. *Proc Natl Acad Sci U S A* **105**, 15299-15304 (2008).
45. Rippa, V. et al. Preferential DNA damage prevention by the E. coli AidB gene: A new mechanism for the protection of specific genes. *DNA Repair (Amst)* **10**, 934-941 (2011).
46. Xiao, Y., Bowen, C. H., Liu, D. & Zhang, F. Exploiting nongenetic cell-to-cell variation for enhanced biosynthesis. *Nat Chem Biol* **12**, 339-344 (2016).
47. Blazeck, J. et al. Harnessing Yarrowia lipolytica lipogenesis to create a platform for lipid and biofuel production. *Nat Commun* **5**, 3131 (2014).

48. Oud, B., van Maris, A. J., Daran, J. M. & Pronk, J. T. Genome-wide analytical approaches for reverse metabolic engineering of industrially relevant phenotypes in yeast. *FEMS Yeast Res* **12**, 183-196 (2012).
49. Yu, X., Liu, T., Zhu, F. & Khosla, C. In vitro reconstitution and steady-state analysis of the fatty acid synthase from Escherichia coli. *Proc Natl Acad Sci U S A* **108**, 18643-18648 (2011).
50. Liu, Z. et al. In Vitro Reconstitution and Optimization of the Entire Pathway to Convert Glucose into Fatty Acid. *ACS Synth Biol* **6**, 701-709 (2017).
51. Clomburg, J. M. et al. Integrated engineering of beta-oxidation reversal and omega-oxidation pathways for the synthesis of medium chain omega-functionalized carboxylic acids. *Metab Eng* **28**, 202-212 (2015).
52. Xu, P., Li, L., Zhang, F., Stephanopoulos, G. & Koffas, M. Improving fatty acids production by engineering dynamic pathway regulation and metabolic control. *Proc Natl Acad Sci U S A* **111**, 11299-11304 (2014).
53. Liu, D., Xiao, Y., Evans, B. S. & Zhang, F. Negative feedback regulation of fatty acid production based on a malonyl-CoA sensor-actuator. *ACS Synth Biol* **4**, 132-140 (2015).
54. Reis, A. C. et al. Simultaneous repression of multiple bacterial genes using nonrepetitive extra-long sgRNA arrays. *Nat Biotechnol* (2019).
55. Larson, M. H. et al. CRISPR interference (CRISPRi) for sequence-specific control of gene expression. *Nat Protoc* **8**, 2180-2196 (2013).
56. Bikard, D. et al. Programmable repression and activation of bacterial gene expression using an engineered CRISPR-Cas system. *Nucleic Acids Res* **41**, 7429-7437 (2013).
57. Engler, C., Kandzia, R. & Marillonnet, S. A one pot, one step, precision cloning method with high throughput capability. *PLoS One* **3**, e3647 (2008).
58. Schirmer, A., Rude, M. A., Li, X., Popova, E. & del Cardayre, S. B. Microbial biosynthesis of alkanes. *Science* **329**, 559-562 (2010).
59. Cao, Y. X. et al. Heterologous biosynthesis and manipulation of alkanes in Escherichia coli. *Metab Eng* **38**, 19-28 (2016).
60. Zhang, F., Carothers, J. M. & Keasling, J. D. Design of a dynamic sensor-regulator system for production of chemicals and fuels derived from fatty acids. *Nat Biotechnol* **30**, 354-359 (2012).

Acknowledgements

This work was supported by the National Key Research and Development Program of China (2018YFA0901300), the National Natural Science Foundation of China (NSFC

21621004), and the Young Elite Scientists Sponsorship Program by Tianjin (TJSQNTJ-2018-16).

Author contributions

L.F., Y.C. and H.S. conceived and designed the experiments. L.F., J.F., and C.W. performed the plasmids construction experiments. L.F. and J.F. performed the fed-batch fermentation experiments. L.F. and Y.C. analyzed the data. L.F. and Y.C. and H.S. wrote the manuscript. H.S. supervised all aspects of the study.

Additional information

Competing interests: The authors declare no competing financial interests.

Figures

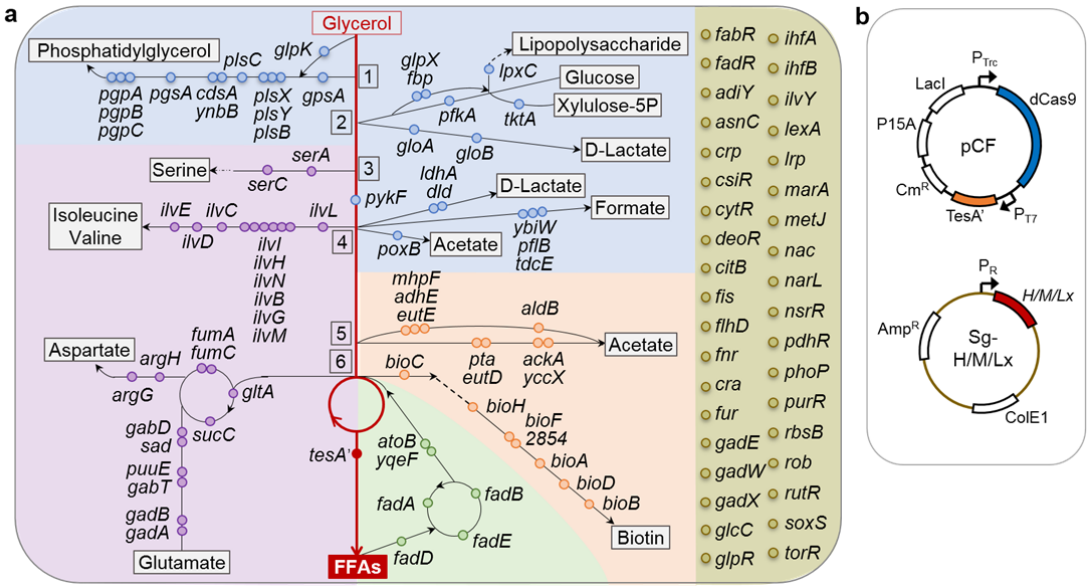

Fig. 1 The CRISPRi approach for identification of beneficial knockdown gene targets from cellular pathways associated with the FFAs metabolism. **a** Schematic of the metabolic or regulatory pathways related to FFAs biosynthesis in *E. coli*, which were classified into five modules (upstream carbon flux diversion, downstream carbon flux diversion, amino acid metabolism, beta-oxidation and transcription factors) and represented in blue, orange, purple, green and golden background, respectively. Genes in the above five modules are shown in italics and marked with blue, orange, purple, green and golden dot, respectively. *2854* represents gene numbered ECD_02854 in BL21(DE3). The fatty acid biosynthetic pathway is shown in red line and key metabolites glycerone-P, glyceraldehyde-3P, glycerate-3P, pyruvate, acetyl-CoA and malonyl-ACP are represented as number 1 to 6, respectively. **b** Plasmid constructs for the gene expression of *tesA'*, *dCas9* and synthetic sgRNAs.

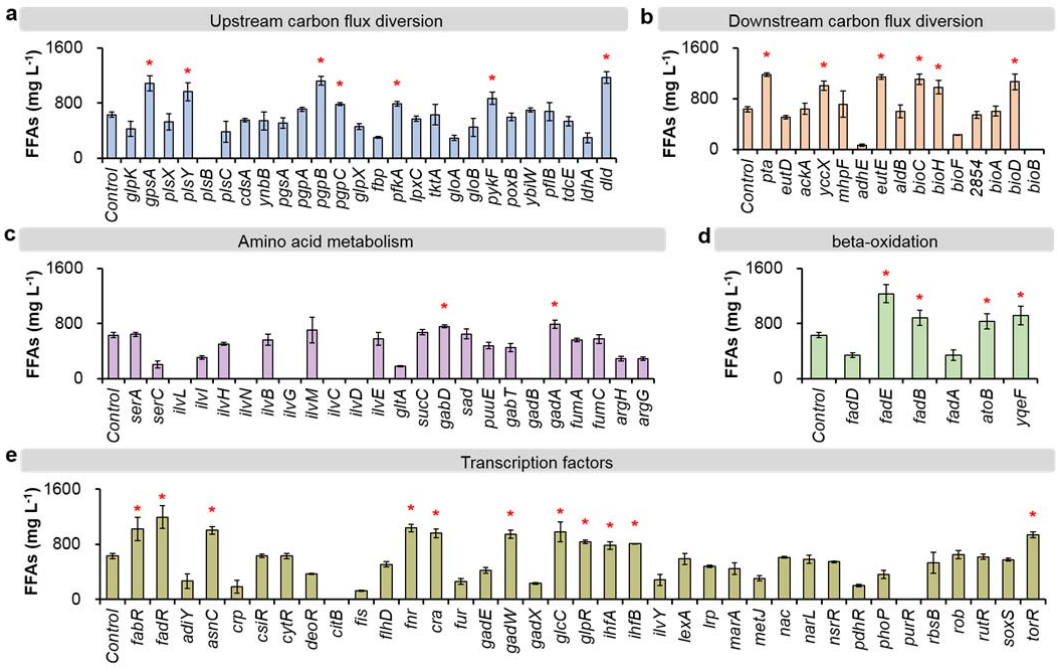

Fig. 2 Effect of genetic perturbation by CRISPRi on FFAs production. FFAs production through repression of each gene in upstream carbon flux diversion module (**a**), downstream carbon flux diversion module (**b**), amino acid metabolism module (**c**), beta-oxidation module (**d**), and transcription factors module (**e**) by the CRISPRi system. All target genes were repressed with high efficiency. * represents the strains with more than 20% increase in FFAs production than that of the strain Control (631 mg L^{-1}). Error bars indicate the standard deviations of three replicates. Source data are provided as a Source Data file

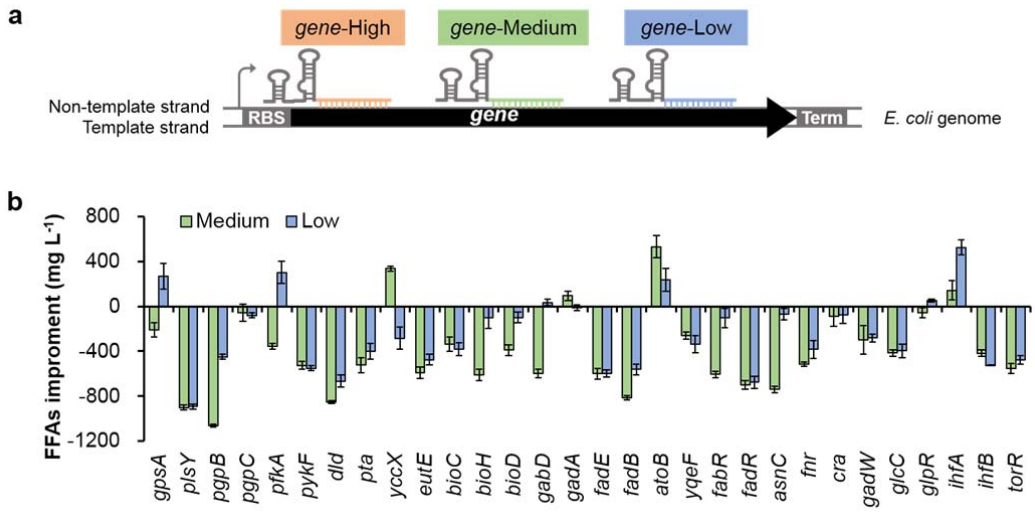

711

712 **Fig. 3** Effect of tuning repression efficiency towards target genes on FFAs production.

713 **a** Design of sgRNA with high, medium or low repression efficiency towards target

714 gene. **b** FFAs production under medium or low repression efficiency compared with

715 that of the high repression efficiency. The repressed genes were screened out from

716 those genes marked with star in Fig. 2. Error bars indicate the standard deviations of

717 three replicates. Source data are provided as a Source Data file

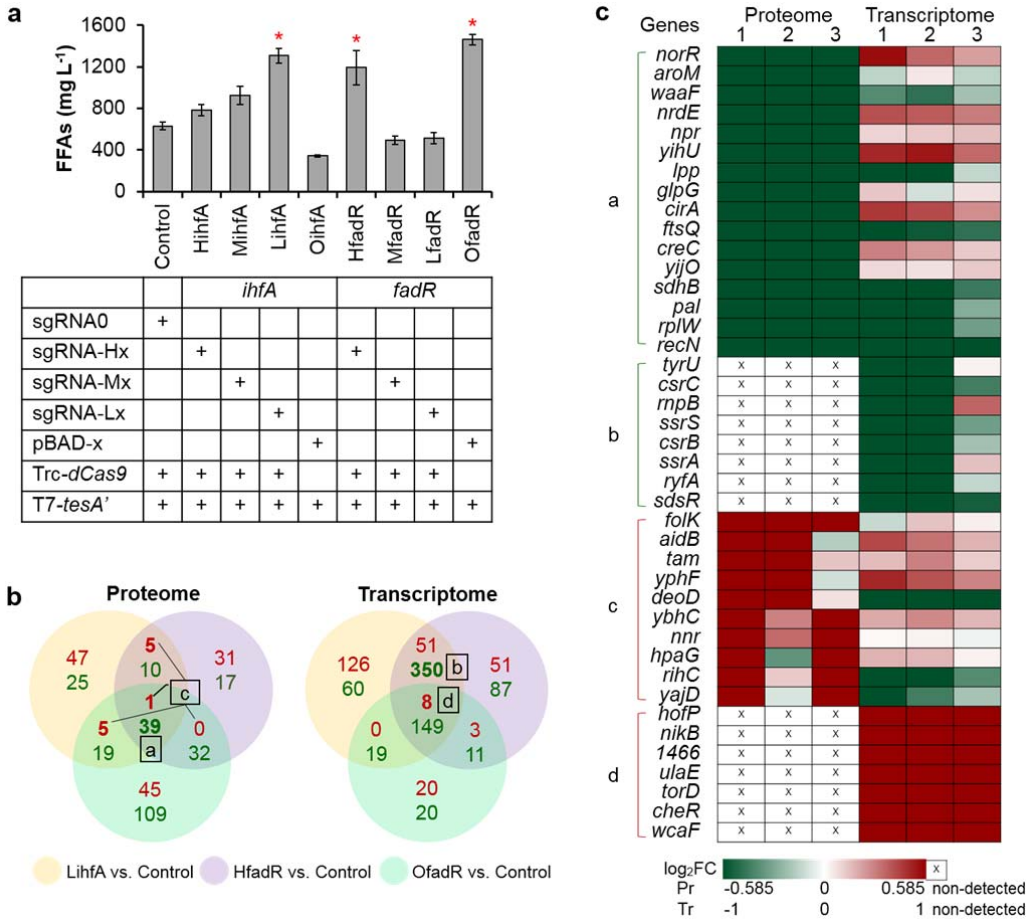

Fig. 4 Exploration of potential target genes by proteome and transcriptome analyses. **a** Effect of different *ihfA* or *fadR* expression levels on FFAs production. * represents the strains with high production of FFAs, and these strains were applied to the next omics analyses. **b** A Venn diagram of differentially expressed genes (DEGs). Common DEGs in the high-titer strains at the protein level (a, c) or at the transcript level (b, d) were identified, compared with the strain Control. Green: down-regulated; red: up-regulated. **c** Expression levels of the selected common DEGs in the strains LihfA (1), HfadR (2), and OfadR (3) compared with the strain Control. *1466*

727 represents the gene numbered ECD_01466 in BL21(DE3). Error bars indicate the

728 standard deviations of three replicates. Source data are provided as a Source Data file

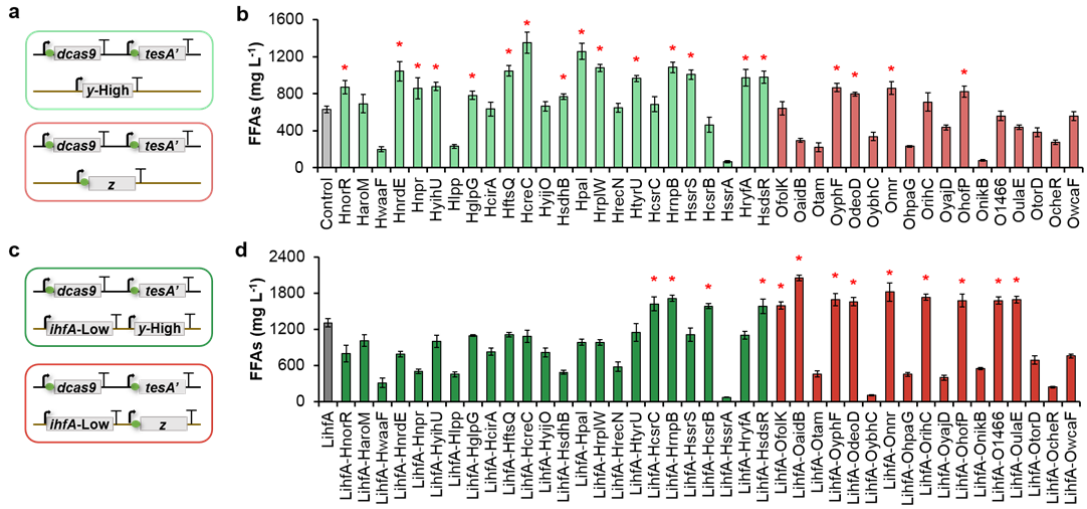

Fig. 5 Reverse engineering of the selected DEGs in the strains CF and LihfA. Schematic of cassettes used to repress or overexpress the selected DEGs in the strain CF (**a**), or in the strain LihfA (**c**). The repression was achieved by CRISPRi and the overexpression was enabled by the P_{BAD} promoter. TesA', dCas9 and sgRNAs were controlled by the P_{T7}, P_{Trc} and P_R promoter, respectively. *y*: down-regulated gene; *z:* up-regulated gene. Effect of genetic perturbation of the selected DEGs on FFAs production in the strain CF (**b**) or in the strain LihfA (**d**). * represents the strain with FFAs titer increased >20% compared with the reference strain in each bar chart. Green frame or column: repression; red frame or column: overexpression. Error bars indicate the standard deviations of three replicates. Source data are provided as a Source Data file

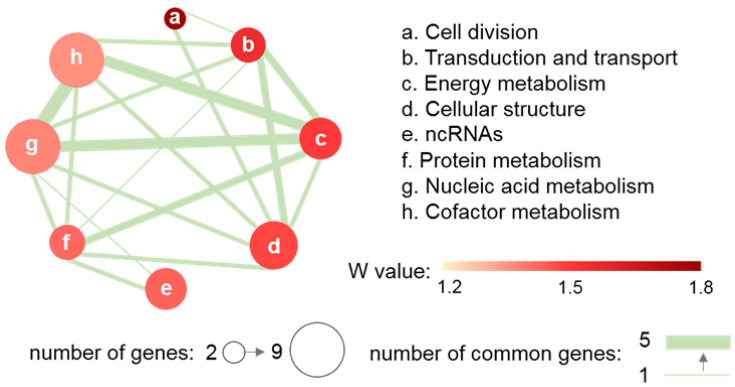

741

742 **Fig. 6** Function network plot of the beneficial genes derived from omics analyses. The

743 size of the node represents the number of genes within the function set. The node's

744 color represents W value of the function set. The thickness of the edge indicates the

745 number of genes overlapping two function sets. W value is calculated by averaging

746 the FFAs ratio of Hx (Ox) / Control or LiHx (LiOx) / LihfA, x referring to each gene

747 belongs to the function set. Genes and the FFAs ratio are shown in Supplementary

748 Table 1. Source data are provided as a Source Data file

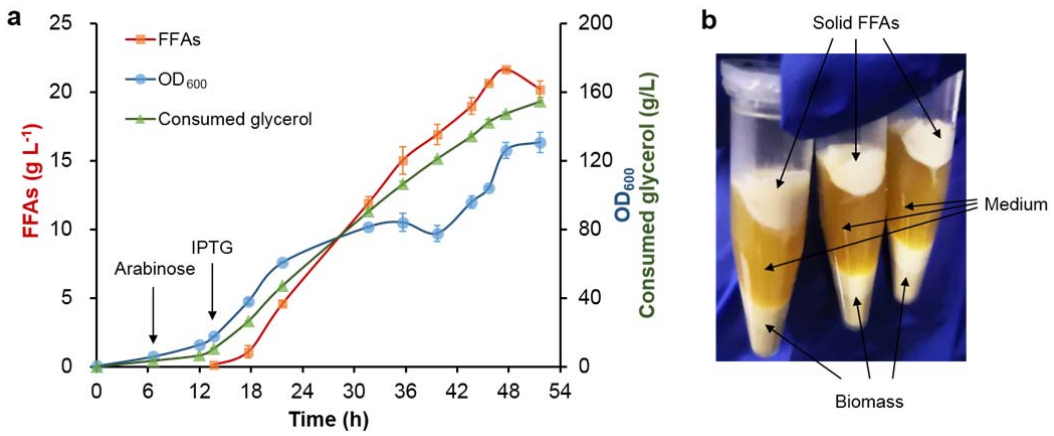

749

750 **Fig. 7** Fed-batch production of FFAs in a 5 L bioreactor. **a** Growth, glucose

751 consumption and FFAs production of the recombinant *E. coli* strain LihfA-OaidB

752 during fed-batch fermentation. **b** Solid FFAs layer after centrifugation. After

753 fermentation, 1 ml of sample was picked up and centrifuged at 5000 g for 10 min.

754 Error bars indicate the standard deviations of three replicates. Source data are

755 provided as a Source Data file